



**HAL**  
open science

## Accurate determination of plutonium by Controlled Potential Coulometry: uncertainty evaluation by the Monte Carlo Method approach

Sebastien Picart, Marielle Crozet, Giacomo Canciani, Ygor Davrain, Daniele Roudil

► **To cite this version:**

Sebastien Picart, Marielle Crozet, Giacomo Canciani, Ygor Davrain, Daniele Roudil. Accurate determination of plutonium by Controlled Potential Coulometry: uncertainty evaluation by the Monte Carlo Method approach. *Journal of Radioanalytical and Nuclear Chemistry*, 2020, 324 (2), pp.747-758. 10.1007/s10967-020-07085-w . cea-03045985v2

**HAL Id: cea-03045985**

**<https://cea.hal.science/cea-03045985v2>**

Submitted on 26 Jun 2024

**HAL** is a multi-disciplinary open access archive for the deposit and dissemination of scientific research documents, whether they are published or not. The documents may come from teaching and research institutions in France or abroad, or from public or private research centers.

L'archive ouverte pluridisciplinaire **HAL**, est destinée au dépôt et à la diffusion de documents scientifiques de niveau recherche, publiés ou non, émanant des établissements d'enseignement et de recherche français ou étrangers, des laboratoires publics ou privés.

1 **Accurate determination of plutonium by Controlled**  
2 **Potential Coulometry: uncertainty evaluation by the**  
3 **Monte Carlo Method approach**

4 Names of the authors: Sébastien Picart, Marielle Crozet, Giacomo Canciani, Ygor Davrain,  
5 Louis Faure, Danièle Roudil.

6 Title: Accurate determination of plutonium by Controlled Potential Coulometry:  
7 uncertainty evaluation by the Monte Carlo Method approach

8 Affiliation(s) and address(es) of the author(s): CEA, DEN, DMRC, Univ Montpellier,  
9 Marcoule, France,

10 E-mail address of the corresponding author: [sebastien.picart@cea.fr](mailto:sebastien.picart@cea.fr)

11

12 **Accurate determination of plutonium by Controlled**  
13 **Potential Coulometry: uncertainty evaluation by the**  
14 **Monte Carlo Method approach**

15 Sébastien Picart, Marielle Crozet, Giacomo Canciani, Ygor Davrain, Louis Faure,  
16 Danièle Roudil.

17 *CEA, DEN, DMRC, Univ Montpellier, Marcoule, France*

18 **Abstract**

19 The accurate determination of plutonium (Pu) mass fraction in nuclear materials is essential  
20 to nuclear matter accountancy and international safeguard programs. Controlled-Potential  
21 Coulometry (CPC) is one of the best available analytical methods to perform such  
22 measurements. The implementation of CPC at the Nuclear Matter Metrological Laboratory  
23 of the French Atomic Energy Commission (CEA) is described as well as the evaluation of  
24 measurement uncertainty using two approaches: the Guide to the expression of uncertainty  
25 in measurement (GUM), and the Monte Carlo Method (MCM). The uncertainty values  
26 determined are compared to the international target values published by the International  
27 Atomic Energy Agency (IAEA).

28 **Keywords**

29 coulometry, plutonium, accuracy, uncertainty, Monte Carlo Method

30

31

32

33        **Introduction**

34        The accurate determination of Pu mass fraction, in both nuclear materials and the spent  
35        fuel reprocessing cycle, is rendered mandatory due to the high accountability required by  
36        the element's fissile nature. Indeed, nuclear organizations must always demonstrate an  
37        effective assessment of criticality and proliferation risks. As such, companies and  
38        institutions working with Pu need Certified Reference Materials (CRMs) in order to  
39        validate their analytical methods, calibrate equipment, and, above all, perform reliable and  
40        accurate content determinations. The production of such CRMs requires highly accurate  
41        methods for characterizing and certifying Pu content.

42        The techniques most commonly used for the determination of Pu with high levels of  
43        accuracy are Isotope Dilution Thermo-Ionization Mass Spectrometry (ID-TIMS), redox  
44        titrimetry, and Controlled-Potential Coulometry (CPC). Of these three techniques, ID-  
45        TIMS uses a spike of enriched Pu to achieve measurements with uncertainties ranging  
46        between 0.17 and 0.28% using very low quantities of Pu (10-50 ng per sample) - in  
47        compliance with the International Target Values (ITVs-2010) published by the IAEA in  
48        2010 [1]- whilst titrimetry bases itself on redox potentiometry and attains comparable  
49        levels of uncertainty (0.21-0.28%, as reported both in literature [2] and in the ITVs-2010)  
50        using a larger amount of Pu material (5-60 mg). CPC, however, displays a vastly better  
51        performance for Pu determination, with measurement uncertainties not exceeding 0.1% [3-  
52        5] for plutonium quantities in the order of 4-15 mg.

53        The particularly low uncertainties of CPC can be attributed to the primary nature of the  
54        analytical method [6]. Unlike ID-TIMS, CPC is not related to chemical standards but only  
55        to physical parameters such as time and current, which can be calibrated with higher  
56        accuracies [7]. Beyond the low uncertainties, it is also important to note that CPC can be  
57        performed on small quantities of analyte [8] (typically, during routine analyses only a few  
58        milligrams of matter are used) and that it is a relatively facile technique to implement.  
59        These advantages have made CPC a particularly interesting technique for metrology  
60        laboratories which provide Pu CRMs such as the CEA's Commission for the Establishment  
61        of Analytical Methods (CETAMA).

62 Fundamentally, CPC is based on the measurement of a quantity of electricity,  $Q$ , involved  
63 in an electrochemical reaction (either oxidation or reduction) and is governed by Faraday's  
64 law, which links the quantity of electricity to the quantity of an element in solution:

$$65 \quad m = Q M / (nF)$$

66 Where  $m$  is the mass of the studied element in g,  $M$  is the molar mass of the element  
67 ( $M=239.075$  g/mol for the Pu sample of interest),  $n$  is the number of electrons exchanged  
68 during the electrochemical reaction ( $n=1$  in the case of the Pu(IV)/Pu(III) redox pair), and  
69  $F$  is Faraday's constant (96485.33212 C/mol) [9].

70 Experimentally,  $Q$  is measured by integrating the current flowing during the oxidation of  
71 Pu(III) into Pu(IV). In order to obtain a selective reaction, it is necessary to work with a  
72 controlled potential applied by a potentiostat in combination with a three electrode  
73 electrochemical set-up. The working electrode material and the electrolyte must be  
74 carefully chosen in order to minimize interferences. In the case of Pu, a gold electrode, a  
75 pure Pu nitrate solution, and a 0.9 mol/L nitric acid electrolyte are recommended [8]. As  
76 every step of the procedure, from sample preparation to signal integration, contributes to  
77 the overall uncertainty of the final measurement result, these steps must be carefully  
78 controlled and optimized when seeking a high degree of accuracy. As such, an appropriate  
79 understanding and calculation of the uncertainties involved in the technique is essential if  
80 CPC analysis is to be performed at high accuracies.

81 The present work aims to achieve a deeper understanding of the technique as well as  
82 providing a method for the treatment of the uncertainties involved in CPC analysis. The  
83 study recalls the key points of the method and discusses the uncertainty budget estimations  
84 through the GUM [10] and the Monte Carlo Method (MCM) approaches [11, 12]. The  
85 MCM method has the advantage of avoiding assumptions with regards to the distribution  
86 law of the measurement result. Through this approach, this work gives an evaluation of the  
87 performance (trueness and precision) of CPC analysis for Pu determination at the  
88 CETAMA's metrological laboratory of Nuclear Matter (LAMMAN).

89

## 90 **Experimental and Methods**

91 Chemicals

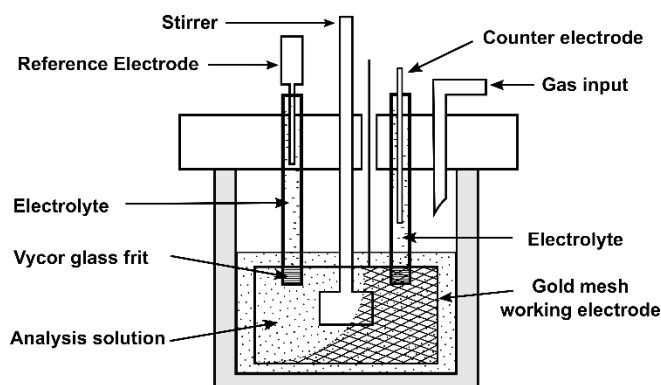
92 All chemical reagents were of analytical grade, concentrated nitric acid (Merck, 65%  
93 Suprapur), concentrated sulfuric acid (Merck, 95-97% for analysis), sulfamic acid (Merck,  
94 Emsure,  $\geq 99.0\%$ ), and hydrogen peroxide (Merck, 30%, Suprapur).

95 All diluted solution were prepared using deionized water (resistivity  $> 18 \text{ M}\Omega \text{ cm}$ ).

96 Pu solutions were prepared by diluting an “EQRAIN Pu N°14” standard solution of Pu  
97 nitrate provided by the CETAMA’s LAMMAN (vial # S007) and are traceable to the MP2  
98 Pu metal certified reference material (CRM). The reference value of Pu mass fraction in  
99 the sample is  $(5.5326 \pm 0.0066) \text{ g/kg}$  (uncertainty determined with a coverage factor  $k=2$ )  
100 on the date of fabrication (March 20<sup>th</sup> 2017). The “EQRAIN Pu N°14” solution density is  
101  $(1144.64 \pm 0.12) \text{ kg/m}^3$  ( $k=2$ ) at 20°C. To calculate the molar mass of Pu at the date of  
102 analysis (May 2018), the MP2 isotopy and the Pu isotope’s decay were taken into account.  
103 From this, the molar mass was evaluated to be  $(239.07458 \pm 0.00001) \text{ g/mol}$  ( $k=2$ ).

104 Coulometric set-up

105 The electrolysis cell used for CPC consisted of a three-electrode system (EG&G Model  
106 377A coulometry cell system) mounted with a gold-gauze working electrode (Au, 99.99%  
107 pure, manufactured by Heraeus. Germany) with a very large surface area (diameter 3.5 cm,  
108 height 2 cm, four layers of 100 mesh per  $\text{cm}^2$  grid, total surface evaluated at  $(123 \pm 5) \text{ cm}^2$   
109 by cyclic voltammetry performed on a iron standard solution), a saturated calomel  
110 reference electrode (SCE, EG&G Model K007) and a platinum counter-electrode (CE)  
111 made of a mesh welded to a wire (Fig. 1).



112

113

Fig. 1 Coulometric set-up

114

115 Each assay was composed of 30 mL of HNO<sub>3</sub> (0.9 mol/L) to which a few drops of sulfamic  
116 acid (1.5 mol/L, approximately 100 μL) were added.

117 In order to avoid the transport of products between the working electrode and the CE, as  
118 well as to minimize the poisoning of analyzed solutions by the reference electrode filling  
119 solutions, the SCE and CE were placed in electrolytic compartments separate from the  
120 analyzed solution. Vycor® membranes were used to establish an electrolytic junction  
121 between these secondary compartments and the central compartment as well as to ensure  
122 ultra-low leakage rates. The medium of the two separate compartments was the same as  
123 the medium of the assay (HNO<sub>3</sub>, 0.9 mol/L).

124 During analysis, a homogeneous solution was maintained by constant mixing with a  
125 paddle-type stirrer (EG&G Model 377 synchronous stirring motor) made of glass with a  
126 morphology optimized to avoid the risk of splashing. Finally, an argon degassing system  
127 allowed to remove dissolved oxygen from the solution. A bubbler was installed upstream  
128 from the electrochemical cell in order to saturate the gas with water and prevent the  
129 medium from drying out.

130 The electrical component of the CPC set-up consisted of a PAR 263A potentiostat coupled  
131 to a high-precision current integrator previously described by Ruas et al [3]. Calibration of  
132 the analogical-digital converter was performed using a high accuracy resistance (Vishay,  
133 RCK04 model, 20 Ω ± 0.01%) and a high accuracy current generator from AOIP (SN8310  
134 calibrator, from 1 nA to 110 mA with uncertainty of 0.002%) of which the accuracy is  
135 periodically verified.

## 136 Procedure

137 The experimental protocol used during experiments was adapted from the ISO 12183  
138 standard [5] as well as from previous literature studies [3, 8, 13]. It can be expressed by six  
139 stages:

### 140 *Sampling and dilution*

141 In the case of concentrated Pu solution, it may be necessary to perform a dilution by weight  
142 on the sample before analysis in order to weigh a mass greater than 1 g for each aliquot  
143 and therefore limit the weighing relative error to less than 0.01% (standard uncertainty,  
144  $k=1$ ) [5, 13, 14]. Indeed, care must be taken whilst measuring the apparent mass of the  
145 solution aliquot to reach the desired uncertainty target of 0.01%.

146 Weighing was performed on a Metler Toledo XP205 analytical scale with maximum  
147 capacity of 200 g and a Maximum Permissible Error (*MPE*) of 1 mg in the range 0-50 g  
148 and 2 mg in the range 50-200 g.

149 In the present work, a sample with an initial Pu concentration close to 5 g/L was diluted by  
150 weight with HNO<sub>3</sub> (0.9 mol/L) by a factor of approximately 5 prior to analysis (i.e.  
151 approximately 13 mL of standard solution were diluted in 40 mL of 0.9 mol/L HNO<sub>3</sub>).  
152 During the experiment, every measurement performed with the analytical scale was  
153 corrected for air buoyancy in order to avoid a systematic error. For this study, each solution  
154 aliquot had a mass of about 4 g (which is comparable to typical values reported by Holland  
155 and co-workers [14]) and, as such, the equivalent mass of Pu in the aliquot was about 6 mg  
156 (which corresponds to the range of 5-10 mg Pu usually recommended for Pu analysis [13]).

### 157 *Fuming*

158 Samples of the Pu diluted reference solution, prepared as described in the previous step,  
159 were weighed directly in the coulometric glass cells used for analysis by using an analytical  
160 scale. Sulfuric acid (1 ml, 3 mol/L) was added to the coulometric cells in order to stabilize  
161 the Pu in the form of Pu(IV) sulfate crystals and to allow elimination of potential chloride,  
162 fluoride, nitrogen, and volatile organic compound impurities in the solutions as well as to  
163 prevent the formation of insoluble plutonium dioxide [13]. A few drops of hydrogen  
164 peroxide solution (30% v/v) were further added to each cell (approximately 100 µL) to  
165 reduce any Pu(VI) potentially present in solution and adjust Pu oxidation state to IV. The  
166 prepared solutions, left to homogenize and react overnight, were finally fumed to dryness  
167 under a nitrogen gas sweep.

168 Furthermore, it is important to note that the conversion of the Pu into Pu(SO<sub>4</sub>)<sub>2</sub> allows to  
169 generate salts which can be redissolved easily in molar nitric acid [15, 16] prior to analysis.



170 *Electrical calibration*

171 A calibration of the analog-to-digital converter used for current integration was performed  
172 by a high precision current calibrator and allowed to apply appropriate corrections to the  
173 reading of integrated current measured during experiments.

174 *Electrode pre-treatment*

175 The gold working electrode was stored in 8 mol/L nitric acid when not in use.  
176 Prior to analysis, a pre-treatment was applied to the working-electrode in a supporting  
177 electrolyte of nitric acid (0.9 mol/L) combined with a small quantity (two drops,  
178 approximately 100  $\mu$ L) of sulfamic acid. This pre-treatment consisted in conducting a  
179 series of pulses: oxidation at  $E_1 = E^{\circ} + 320$  mV, reduction at  $E_2 = E^{\circ} - 360$  mV, and oxidation  
180 back to  $E_1$  (where  $E^{\circ}$  is the formal potential of the Pu(IV)/Pu(III) redox pair in  $\text{HNO}_3$   
181 0.9 mol/L) [5].

182 *Blank measurement*

183 A blank was measured in the same medium which served for pre-treatment. The procedure  
184 consisted in a reduction step at  $E_1 = E^{\circ} - 230$  mV followed by an oxidation step at  
185  $E_2 = E^{\circ} + 230$  mV. The duration of oxidation ( $t_1$ ), the residual current ( $i_{r1}$ ), and the raw  
186 quantity of electricity of the blank ( $Q_1$ ) were recorded during the oxidation step. For both  
187 electrochemical steps, the reaction was ended when a stable current of a few  $\mu$ A with a  
188 drift inferior to 1  $\mu$ A over 100 s was recorded. The potentials applied during this phase  
189 were the same as those used for the coulometric analysis of Pu [3].

190 *Analysis of plutonium*

191 The dried test sample was dissolved in the supporting electrolyte used for the blank  
192 measurements.  
193 During analysis measurements, the Pu(IV) in the test sample was first reduced to Pu(III)  
194 by applying a potential  $E_1$  ( $E_1 = E^{\circ} - 230$  mV). The generated Pu(III) solution was then  
195 oxidized back to Pu(IV) by applying a potential  $E_2$  ( $E_2 = E^{\circ} + 230$  mV). During the two

196 electrochemical processes, the shift in applied potential from  $E^{\circ'}$  of 230 mV was chosen  
 197 in order to ensure the almost complete conversion of Pu at equilibrium (close to 99.99%)  
 198 whilst avoiding the reactions of interfering species. The current measured during the  
 199 oxidation phase was integrated as a function of time until the same stopping criteria as  
 200 those used for the measurement of the blank (a stable current of a few  $\mu\text{A}$  with a drift  
 201 inferior to 1  $\mu\text{A}$  over 100 s) were reached. During this second phase, the duration of  
 202 oxidation ( $t_2$ ), the residual current ( $i_{r2}$ ), and the raw quantity of electricity ( $Q_2$ ) spent during  
 203 the phase, were recorded.

204 The net quantities of electricity, for the blank and the sample (noted as  $Q_b$  and  $Q_s$ ,  
 205 respectively) were calculated from the raw quantities of electricity  $Q_1$  and  $Q_2$ , by  
 206 subtracting of the quantity of electricity due to the residual currents from the raw quantity  
 207 of electricity (as shown in Eq. (1) and (2) for  $Q_b$  and  $Q_s$ , respectively):

$$208 \quad Q_s = Q_2 - i_{r2}t_2 \quad (1)$$

$$209 \quad Q_b = Q_1 - i_{r1}t_1 \quad (2)$$

210 By incorporating  $Q_s$  and  $Q_b$  in Faraday's law, the mass of Pu in the studied sample can be  
 211 expressed as shown in Eq. (3):

$$212 \quad m_{\text{Pu}} = (Q_s - Q_b)M_{\text{Pu}} / (nFf) \quad (3)$$

213 A correction factor,  $f$ , which accounts for the fractions of Pu not electrolyzed during the  
 214 analysis is also introduced in Eq. (3).  $f$  takes into account the amount of Pu(IV) not reduced  
 215 during first stage of the analyses and that of Pu(III) not oxidized during the second stage  
 216 of the analyses. It is dependent on potentials applied and calculated by applying Nernst  
 217 Law (taking the assumption that the system has reached equilibrium).  $f$  is expressed as  
 218 shown in Eq. (4):

$$219 \quad f = \frac{\exp\left(\frac{n \cdot F \cdot (E_2 - E^{\circ'})}{R \cdot T}\right)}{1 + \exp\left(\frac{n \cdot F \cdot (E_2 - E^{\circ'})}{R \cdot T}\right)} - \frac{\exp\left(\frac{n \cdot F \cdot (E_1 - E^{\circ'})}{R \cdot T}\right)}{1 + \exp\left(\frac{n \cdot F \cdot (E_1 - E^{\circ'})}{R \cdot T}\right)} \quad (4)$$

220 In Eq. (4),  $E_2$  and  $E_1$  are the potentials applied for the oxidation and reduction phases,  
 221 respectively;  $E^{\circ'}$  is the formal potential of the Pu(IV)/Pu(III) redox pair;  $n$  is the number  
 222 of electrons exchanged (equal to 1 for the studied system);  $F$  is Faraday's constant;  $R$  is the  
 223 molar gas constant (equal to 8.3144598 J mol<sup>-1</sup> K<sup>-1</sup> [9]); and  $T$  is the temperature of the  
 224 studied system (in K).

225 Although the value of  $f$  is very close to 1, typically 0.9997, it is indispensable to take into  
226 account in order to achieve high accuracy.

227 Monte Carlo Method simulation

228 The MCM calculations were run using the JMP ®13.0.0 software developed by SAS  
229 Institute Inc. using a random draw of 1,000,000. From the mathematical expressions of  $Pu$   
230 mass fraction and  $f$ , the probability density function was calculated for those terms using  
231 the parameters input of each variable (value, standard uncertainty, and assumed  
232 distribution).

## 233 **Results and Discussion**

234 Sample weighing

235 The weight measurements performed for sampling and dilution of the concentrated Pu  
236 solution (considered hereafter as the stock solution) during this experiment are presented  
237 in Table 1. In the table, the mass of the stock and diluted solutions are given both as read  
238 and as corrected for air buoyancy. The  $K$  factor used for air buoyancy correction is  
239 described in Eq. (5):

$$240 \quad K = \frac{\left(1 - \frac{\rho_{air}}{\rho_{std}}\right)}{\left(1 - \frac{\rho_{air}}{\rho_{sol}}\right)} \quad \text{with} \quad m_{corrected} = K \times m_{as\ read} \quad (5)$$

241 In Eq. (5),  $\rho_{air}$  is the air density which is dependent of temperature, relative humidity and  
242 pressure recorded during experiment (in this study, conditions in glove box were: pressure  
243 = 100450 Pa, relative humidity = 59,6% and temperature = 19,0°C giving  $\rho_{air}$ =  
244 1.1925 kg/m<sup>3</sup>),  $\rho_{std}$  is the density of the inox standard used for the scale calibration  
245 (8010 kg/m<sup>3</sup>),  $\rho_{sol}$  is the density of the weighed solution.

246 A systematic mass measurement error (bias between 0.09% and 0.10%) was observed,  
247 which demonstrates that at the level of uncertainty desired, the correction for air buoyancy  
248 is not negligible for a solution which density is close to 1000 kg/m<sup>3</sup> (and is, in fact,  
249 essential). By contrast, the air buoyancy correction uncertainty will be neglected in the

250 global calculation of mass measurement uncertainty as it was estimated to be 0.0002% and  
 251 found insignificant by Cordaro and coworkers [13].

	EQRAIN solution	Diluted EQRAIN solution
m(tare) (g)	133.35252	148.46070
m(tare+solution) (g)	148.46070	189.52380
m(solution) as read (g)	15.10823	56.17128
density (kg/m <sup>3</sup> )	1144.64	1057,0
m(solution) corrected (g)	15.12173	56.22635

252 **Table 1** Weight measurements of stock and diluted solutions, both the gross data and  
 253 that corrected for air buoyancy are reported

### 254 Dilution factor calculation

255 By using the masses of the EQRAIN ( $m_{EQRAIN}$ ) and diluted EQRAIN ( $m_{dil. EQRAIN}$ ) solutions  
 256 (corrected for air buoyancy), a dilution factor,  $DF$ , was evaluated as expressed in Eq. (6).

$$257 \quad DF = \frac{m_{dil. EQRAIN}}{m_{EQRAIN}} \quad (6)$$

258 The relative standard uncertainty on  $DF$ ,  $u_r(DF)$ , was expressed as shown in Eq. (7),  
 259 considering that the standard uncertainty for mass values between 50 and 200 g is equal to  
 260  $MPE$  ( $MPE = 2$  mg) divided by  $\sqrt{3}$  (uniform distribution law).

$$261 \quad u_r(DF) = \sqrt{u_r^2(m_{EQRAIN}) + u_r^2(m_{dil. EQRAIN})} = \frac{1}{\sqrt{3}} \sqrt{\left(\frac{MPE}{m_{EQRAIN}}\right)^2 + \left(\frac{MPE}{m_{dil. EQRAIN}}\right)^2} = 0.008\% \quad (7)$$

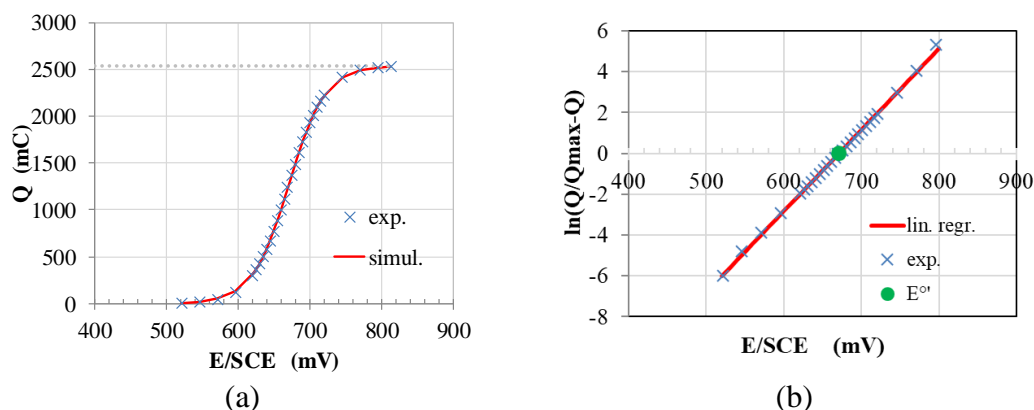
262 In Eq. (7),  $u_r^2(m_{EQRAIN})$  and  $u_r^2(m_{dil. EQRAIN})$  are the relative variance of  $m_{EQRAIN}$  and  
 263  $m_{dil. EQRAIN}$  respectively,  $m_{EQRAIN} = 15121.73$  mg,  $m_{dil. EQRAIN} = 56226.35$  mg and  $MPE =$   
 264 2 mg.

265 From Eq. (6) and (7),  $DF$  was determined to be  $3.71825 \pm 0.00059$  ( $k=2$ ) for this experiment.

### 266 Measurement of the Pu(IV)/Pu(III) formal redox potential

267 The determination of the formal potential ( $E^{\circ'}$ ) value in the same conditions as the CPC  
 268 titration (using a gold electrode and a 0.9 mol/L  $HNO_3$  medium) is required in order to  
 269 calculate the corrective factor  $f$ .  $E^{\circ'}$  was determined from a series of five coulograms, the  
 270 results of which are reported in Table 4. Coulograms are plots of the quantity of electricity,

271  $Q$ , necessary to reach equilibrium (i.e. low current) from a completely reduced solution in  
 272 function of the potential applied to the working electrode,  $E$ . The inflexion point of the  
 273 curve observed in a coulogram corresponds to the studied couple's  $E^{\circ'}$ , a potential at which  
 274 there is as much oxidizer Pu(IV) as there is reducer Pu(III). This inflexion point is  
 275 determined by plotting  $\ln(Q/Q_{max}-Q)$  vs.  $E$  (where  $Q_{max}$  is the maximum value of  $Q$ ) and  
 276 determining the  $x$ -intercept of the linear regression of the plotted curve. An example of the  
 277 determination of  $E^{\circ'}$  for a given experiment is presented in Fig. 2.



278 **Fig. 2** Coulogram of experiment LF06 for a Pu nitrate solution in 0.9 mol/L HNO<sub>3</sub> and  
 279 a small amount of sulfamic acid. In both graphs the experimental values are represented  
 280 by the crosses whilst the lines show the simulation of the data calculated according to  
 281 the Nernst law (a) and the linear regression used to determine  $E^{\circ'}$  (b)

282 The mean value of  $E^{\circ'}$  ( $671 \pm 4$ ) mV/SCE of the Pu(IV)/Pu(III) couple calculated from  
 283 coulograms during the present study is shown in Table 2 in relation to the values reported  
 284 in literature for comparable media. It can be seen that the  $E^{\circ'}$  determined during this series  
 285 of experiments is consistent with the previously reported values, demonstrating the validity  
 286 of using coulograms for the determination of  $E^{\circ'}$  under the chosen experimental conditions.

$E^{\circ'}$ (Pu(IV)/Pu(III)) mV/SCE	Electrolyte	Ref.	T °C
690	HNO <sub>3</sub> 1M	[16]	room T
674.2	HNO <sub>3</sub> 1M	[17]	room T
677	HNO <sub>3</sub> 0.9M	[8]	25
$673 \pm 5$	HNO <sub>3</sub> 0.9M	[3]	room T
$678 \pm 6$	HNO <sub>3</sub> 1M	[18]	25
$682 \pm 10$	HNO <sub>3</sub> 1M	[19]	25
668	HNO <sub>3</sub> 0.9M	[5]	

671±4	HNO3 0.9M	This work	24
-------	-----------	-----------	----

287 **Table 2** Comparison of Pu(IV)/Pu(III) formal potentials in aqueous nitric acid  
 288 solutions (with concentrations close to 1 mol/L, in mV/SCE) from literature with the  
 289 value calculated during the present study

### 290 Blank repeatability

291 As discussed previously, the quantity of electricity of the blank,  $Q_b$ , needs to be taken into  
 292 account as a corrective factor during analysis. In order to establish the precision of  $Q_b$  in  
 293 repeatability conditions, a series of 8 consecutive measurements was recorded for a single  
 294 experiment (LF01). The mean value of  $Q_b$  (12.2 mC) and its standard uncertainty ( $u(Q_b) =$   
 295 0.7 mC) over the 8 measurements are reported in Table 3 in addition to the specific details  
 296 for each measurement.

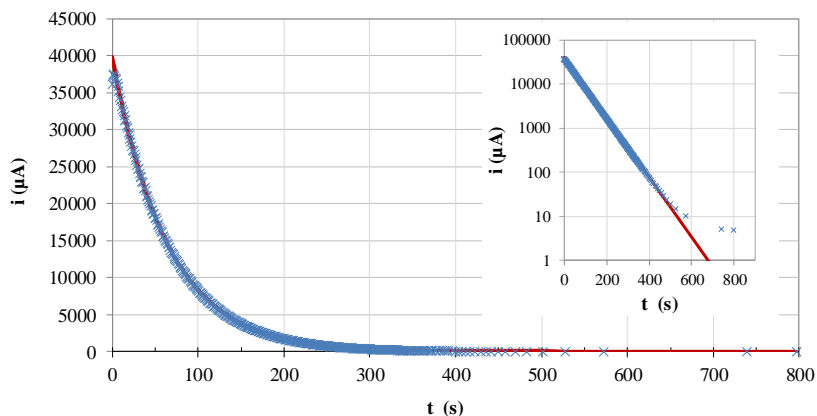
replicates	1	2	3	4	5	6	7	8	Mean value	$u(Q_b)$
$Q_1$ (mC)	12.0	13.7	13.2	13.2	13.1	13.1	12.9	12.9	13.01	0.45
$i_{r1}$ ( $\mu$ A)	3.32	2.11	1.74	1.74	1.40	1.26	1.51	0.96	1.76	0.68
$t_1$ (s)	466	432	436	436	465	393	393	472	437	29
$Q_b$ (mC)	10.5	12.8	12.4	12.4	12.5	12.6	12.3	12.4	12.24	0.69

297 **Table 3** Variations in  $Q_b$  over a series of consecutive measurements

298 It is important to note, at this point, that the blank determination and the control of its  
 299 variability are particularly important during analyses. Indeed, a variation of 1 mC, for  
 300 instance, is representative of 2.5  $\mu$ g Pu and corresponds to  $2.5/6000 = 0.04\%$  of the total  
 301 signal recorded during an analysis.

### 302 Analysis of pure plutonium nitrate solutions

303 Figure 3 shows the evolution of current in the coulometric cell in relation to time during  
 304 the second phase of the Pu analysis (the oxidation of Pu(III) to Pu(IV)). The recorded  
 305 current can be seen to decrease exponentially in relation to time, consistently with the  
 306 typical current response at a working electrode to a potential pulse for a transport regime  
 307 limited by convective diffusion [20].



308

309 **Fig. 3** Plot of the current versus time for the oxidation of a Pu(III) solution at a gold  
 310 electrode during Experiment LF06. The Solid line represents the simulated data, whilst  
 311 the crosses are the experimentally observed values. The insert shows the logarithmic plot  
 312 of current versus time for the same data

313 In reactions limited by convective diffusion, the evolution of current can be expressed as  
 314 shown in Eq. (8) [21]. From this equation, the terms of initial current,  $i_0$ , and cell  
 315 coefficient,  $p$ , can be estimated for an experiment's given analytic conditions (including  
 316 set-up, stirring mode, and nature of the analyte).

$$317 \quad i(t) = i_0 \exp(-pt) \quad (8)$$

318 In Eq. (9), the coefficient cell,  $p$ , is expressed in  $s^{-1}$  and represents the rate of the reaction.  
 319  $p$  is expressed as a function of the surface area of the electrode,  $A$ , the volume of solution,  
 320  $V$ , and the mass transfer coefficient,  $m$ . In a convective diffusion regime,  $m$  is dependent  
 321 on the diffusion coefficient of the Pu species, on the viscosity of the medium, and on the  
 322 stirring speed during experiments.

$$323 \quad p = m \frac{A}{V} \quad (9)$$

324 The inverse value of  $p$  represents the cell constant,  $\tau$  (expressed in seconds). For a duration  
 325 of electrolysis corresponding to  $6.9\tau$ , a proportion of 99.9% of the initial Pu(III) will have  
 326 been oxidized. This calculation provides a good indication of the time of analysis required  
 327 by a CPC titration (at least 500 s).

328 From Eq. (8) and (9), it was possible to determine the terms  $i_0$ ,  $p$ , and  $\tau$  for the experiments  
 329 performed in this study. The values for these terms as determined by the mathematical  
 330 simulations are shown in Table 4 in addition to the  $i_0$ , value measured experimentally. It

331 can be seen that the terms are reproducible between experiments. The mean value of  $p$   
 332 (close to  $15 \cdot 10^{-3} \text{ s}^{-1}$ ) is consistent with values previously reported in literature [21]. As  
 333 such, the stirring procedure in the present study can be considered optimized for the  
 334 specific experimental conditions: sufficient to reach a reasonable rate of reaction without  
 335 risks of splashing.

Experiment	$i_{0 \text{ exp}} (\mu\text{A})$	$i_{0 \text{ sim}} (\mu\text{A})$	$10^3 p (\text{s}^{-1})$	$\tau(\text{s})$	$6,9\tau (\text{s})$
LF04	33788	35025	13.8	72.4	500
LF05	34465	36406	14.4	69.4	479
LF06	36238	39785	15.7	63.9	441
LF07	32448	34814	13.7	72.9	503
LF08	34570	36615	14.5	69.1	477

336 **Table 4** Parameters of the current simulation: cell constant determination for the series of  
 337 experiments

338 Having established the suitability and precision in reproducibility conditions of the  
 339 experimental procedure employed, titrations of five aliquots of the EQRAIN Pu 14  
 340 standard (vial S007) was performed at room temperature ( $24^\circ\text{C}$ ). The Pu mass in the  
 341 studied samples was determined as a function of the quantity of electricity used during the  
 342 analysis (corrected, as written in Eq. (10), for the responses of the residual and blank  
 343 currents as well as the fraction of Pu electrolyzed) as previously described in Eq. (3). It is  
 344 important to note that the molecular mass of Pu in the samples was corrected at the date of  
 345 analysis in order to account for radioactive decay.

$$346 \quad m_{Pu} = \frac{Q}{nFf} M_{Pu} = \frac{(Q_2 - Q_1 - i_{r2}t_2 + i_{r1}t_1)}{nFf} M_{Pu} \quad (10)$$

347 The results of the five analyses are presented in Table 5 and compared to the reference  
 348 mass of Pu (calculated from an equivalent mass of reference solution). The bias on the  
 349 measurements (D%) is calculated from the difference between the experimental and  
 350 reference values, as shown in Eq. (11).

351

$$352 \quad D(\%) = \frac{(m_{exp} - m_{ref})}{m_{ref}} \quad (11)$$

353



Exp	Q <sub>1</sub> (mC)	I <sub>r1</sub> (μA)	t <sub>1</sub> (s)	Q <sub>2</sub> (mC)	I <sub>r2</sub> (μA)	t <sub>2</sub> (s)	E <sup>o'</sup> (Pu <sup>(IV)</sup> /Pu <sup>(III)</sup> ) (mV/SCE)	f	T(°C)	m <sub>Pu</sub> ref. (mg)	m <sub>Pu</sub> exp. (mg)	D(%)
LF04	11.0	3.0	410	2553.2	4.0	865	668.3	0.999739	23.9	6.29319	6.29518	0.032%
LF05	10.4	2.6	431	2546.6	4.5	908	668.3	0.999735	24.3	6.28324	6.27852	-0.075%
LF06	9.3	2.9	381	2561.6	4.8	798	670.8	0.999742	24.0	6.31678	6.31913	0.037%
LF07	12.7	1.6	461	2554.5	2.8	914	673.4	0.999741	24.3	6.30111	6.29521	-0.094%
LF08	9.7	2.3	372	2551.2	3.7	834	672.9	0.999737	24.9	6.29828	6.29357	-0.075%

354 **Table 5** Results, experimental parameters, and calculated bias for the experimental  
 355 determination of Pu mass for EQRAIN Pu 14 standard samples by CPC

356 It can be seen in Table 5 that a bias of less than 0.1% was observed for individual results.

357 This low bias is consistent with the expected performances of CPC [4,5].

### 358 Uncertainty calculations according to GUM

359 The Pu mass fraction [Pu] (in g/kg) in the analyzed samples was determined by the ratio  
 360 between the experimental mass of Pu,  $m_{Pu}$ , and the weight of diluted solution  
 361 (corresponding to the mass of sample corrected for air buoyancy,  $m_{sample}$ ) divided by the  
 362 dilution factor  $DF$ . From this, the Pu mass fraction can be expressed as shown in Eq. (12).

$$363 \quad [Pu] = \frac{m_{Pu}}{m_{sample}} DF = \frac{Q}{nFf} \frac{M_{Pu}}{m_{sample}} DF \quad (12)$$

364 Precision analysis on the Pu mass fraction determination can be carried out by a classical  
 365 GUM approach [10], which consists in applying the law of propagation of variances to the  
 366 mathematical expression of the Pu mass fraction reported in Eq. (12). During GUM  
 367 analysis, only the uncertainties on the parameters  $Q$ ,  $m_{sample}$ , and  $DF$  are taken into account  
 368 as the uncertainties on the  $M_{Pu}$ , and  $f$  parameters can be considered negligible (as discussed  
 369 later in this text).

370 Indeed, uncertainties on  $M_{Pu}$ , and  $f$ , have been estimated according to their probability  
 371 distribution and their standard uncertainty (taken from previous experiments, see Table 6).

372 The uncertainty on  $M_{Pu}$  was taken from the MP2 CRM certificate, considering that the  
 373 uncertainty from radioactive decay between the dates of analysis is non-significant. The  
 374 value of the Faraday constant,  $F$ , was taken from the CODATA publication and is  
 375 considered as a constant since 2019 [9]. Concerning the  $f$  factor, its uncertainty range was  
 376 calculated by experimentally varying the formal potential by  $\pm 5$ mV and measuring its

377 impact on the  $f$  value. This gave a measuring span of 0.006% [22] and a relative standard  
 378 uncertainty of 0.0017% (i.e.  $0.006/(2\sqrt{3})$ ) (considering a uniform distribution).

379

Variable	$u_r$ (k=1)	distribution	Ref.
$M_{Pu}$	$3.8 \cdot 10^{-5} \%$	normal	[23]
$f$	$1.7 \cdot 10^{-3} \%$	uniform	[22]

380

**Table 6** Relative uncertainty evaluations for  $M_{Pu}$ , and  $f$  factors.

381 Eliminating the negligible terms, the expression of the combined relative uncertainty,  $u_r$ ,  
 382 could then be simplified as expressed in Eq. (13). It is important to note that each term in  
 383 Eq. (13) is independent (there are no covariance terms) and must thus be evaluated in order  
 384 to assess the global variance on Pu mass fraction

$$385 \quad u_r^2([Pu]) = u_r^2(Q) + u_r^2(DF) + u_r^2(m_{sample}) \quad (13)$$

386 The variance of  $Q$  terms is difficult to estimate because every Pu coulometric experiment  
 387 is unique and can not be repeated. Thus, in a first approach, we consider that it is  
 388 proportional to the variance of the quantity of electricity of the blank,  $u^2(Q_b)$ , which is the  
 389 best estimator of the uncertainty for the integration of current.

390

391 As such  $u_r(Q)$  can be expressed as shown in Eq. (14):

$$392 \quad u_r^2(Q) = u_r^2(Q_s - Q_b) = \frac{u^2(Q_s - Q_b)}{Q^2} = 2 \frac{u^2(Q_b)}{Q^2} \quad (14)$$

393 Numerically,  $u_r(Q)$  was calculated to be:

$$394 \quad u_r(Q) = \sqrt{2} \frac{u(Q_b)}{Q} = \sqrt{2} \times \frac{0.7}{2500} = 0.040\%$$

395 Concerning the variance of  $m_{sample}$  in Eq. (15), it was estimated from the  $MPE$  of the scale  
 396 in the 0-50 g range (1 mg) and the expected uniform distribution law for weighing:

$$397 \quad u_r^2(m_{sample}) = \frac{1}{3} \frac{MPE^2}{m_{sample}^2} \quad (15)$$

398 Which becomes:

$$399 \quad u_r(m_{sample}) = \frac{1}{\sqrt{3}} \times \frac{1}{4250} = 0.014\%$$

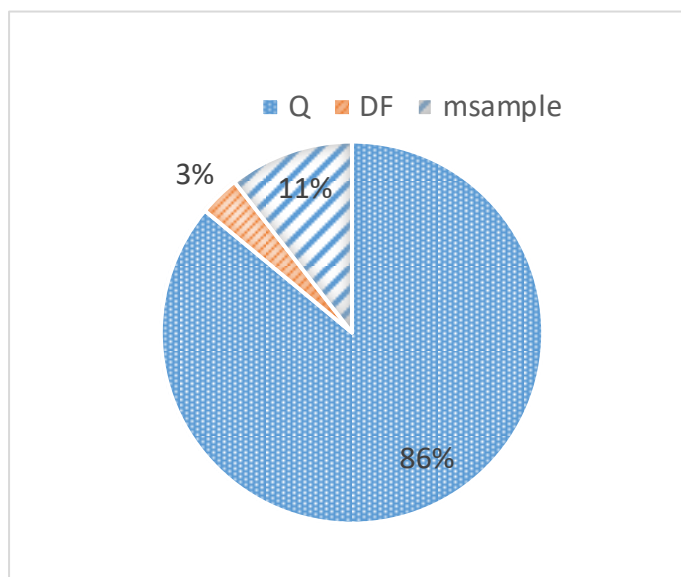
400 The variance on  $DF$  has already been discussed and the numerical value of the relative  
 401 uncertainty is:

402 
$$u_r(DF) = 0.008\%$$

403 The relative standard uncertainty on Pu concentrations is then a combination of these three  
404 variances (cf. Eq. (13)):

405 
$$u_r([Pu]) = \sqrt{0.040^2 + 0.014^2 + 0.008^2} = 0.043\%$$

406 From this, it is possible to calculate each element's contribution to the uncertainty budget.  
407 The major contributor to the uncertainty budget is the measurement of the quantity of  
408 electricity (86%), followed by the contribution of the weighing of the sample (11%) and  
409 that of the dilution factor (3%) (as seen in Fig. 4).



410  
411 **Fig. 4** Uncertainty budget distribution between the measurement of the quantity of  
412 electricity, Q, the dilution factor, DF, and the sample mass,  $m_{\text{sample}}$

413 It can be seen from Fig. 4 that the weighing operations, if they are properly conducted, are  
414 not detrimental to the accuracy of CPC measurements (14% of the uncertainty budget).  
415 However, the quality of the measurement of the quantity of electricity, and, most  
416 importantly, the stability of the blank response, are particularly important to the accuracy  
417 of the performed analytical measurements.

#### 418 Uncertainty calculations by the Monte Carlo Method

419 The Monte Carlo Method (MCM) for the evaluation of measurement uncertainty is based  
420 on the propagation of probability distributions[11, 24, 25]. This method is a practical  
421 alternative to the GUM classical approach and is of greater advantage when:

422 - the measurand mathematical model is complicated and introduces errors due to both  
 423 linearization and difficulty to provide the partial derivatives of the model.  
 424 - the uncertainties of the input variables are not of the same magnitude.  
 425 This approach is actually more appropriate for the estimation of the uncertainties of  $f$  and  
 426  $m_{Pu}$  since their expressions are non-linear and because the uncertainties of the different  
 427 input variables are not of the same order, as one can note in Table 7.

input variables	value	standard uncertainty (k=1)	assumed distribution
$Q_1$ (mC)	11.0	0.5	normal
$i_{r1}$ ( $\mu$ A)	3.0	0.7	normal
$t_1$ (s)	410	1	uniform
$Q_2$ (mC)	2553	0.5	normal
$i_{r2}$ ( $\mu$ A)	4.0	0.8	normal
$t_2$ (s)	865	1	uniform
$M_{Pu}$ (g/mol)	239.07458	0.00001	normal
$F$ (C/mol)	96485.33212	none	
$R$ (J mol <sup>-1</sup> K <sup>-1</sup> )	8.3144598	none	
$T$ (K)	297	1	uniform
$E^{\circ}$ (mV/ECS)	671	2	normal
$E_1$ (mV/ECS)	444.6	0.4	normal
$E_2$ (mV/ECS)	903.8	0.4	normal
$m_{\text{sample}}$ (g)	4.223	0.0006	uniform
$m_{\text{EQRAIN}}$ (g)	15.122	0.0012	uniform
$m_{\text{dil. EQRAIN}}$ (g)	56.226	0.0012	uniform

428 **Table 7** Value, standard deviation, and distribution of input variables for the evaluation  
 429 of measurement uncertainty by MCM (example data from experiment LF04 except for  
 430  $E^{\circ}$  taken equal to the formal potential mean value)

431 For MCM analysis, a great number of parameter values,  $N$ , are sampled at random from  
 432 the distribution of the input quantities. If  $N$  is large enough (usually  $N \geq 10^6$  as  
 433 recommended in the supplement 1 of GUM10), a probability density function for the  
 434 measurement results can be traced. From this probability function, the parameters  
 435 (expectation and variance) can be estimated. With MCM simulations, the coverage interval  
 436 ( $CI$ ) of the distribution comes directly from the probability density function of the

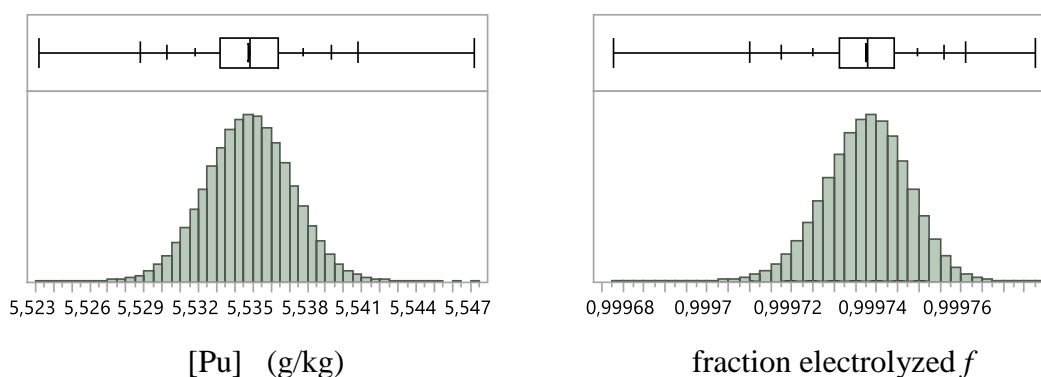
437 measurement result. This is one of the main advantages of MCM when compared to the  
 438 classical GUM approach, where a normal distribution assumption has to be made.

439 For the MCM simulation studies, the full mathematical expression for the Pu mass fraction  
 440 is presented in Eq. (16).

$$441 \quad [Pu] = \frac{Q}{nFf} M_{Pu} \frac{DF}{m_{sample}} = \frac{(Q_2 - Q_1 - i_{r2}t_2 + i_{r1}t_1)}{nFf} M_{Pu} \frac{m_{dileQRAIN}}{m_{EQRAIN} \cdot m_{sample}} \quad (16)$$

442 Using the input parameters of Table 7, the probability density function was thus calculated  
 443 for the [Pu] and  $f$  terms using the JMP software and their profiles were plotted as seen in  
 444 Fig. 5. From these profiles, the coverage intervals are deduced.

445



446 **Fig. 5** Probability density functions and quartiles (shown in the box plots above each  
 447 function) for the Pu concentration (left), and the fraction of Pu electrolyzed (right)  
 448 calculated from Monte Carlo calculations by using the input details presented in Table 7  
 449

Uncertainty Calculation Approach	[Pu]		f	
	$u_r$	$U_r$ or CI	$u_r$	$U_r$ or CI
GUM	0.043 %	0.086 %	0.0017 %	0.0034 %
Monte Carlo Method	0.041 %	0.082 %	0.0006 %	0.0011 %

450 **Table 8** Comparison of uncertainty evaluations between the GUM and MCM approaches.  
 451 The uncertainties calculated through the MCM are shown in Table 8 and compared to those  
 452 calculated previously with the GUM method. It is possible to see that the values of [Pu]  
 453 uncertainties are consistent between the two calculations. As the  $Q_s$  and  $f$  terms are

454 estimated more finely by Monte Carlo Method, the GUM approach tends to overestimate  
 455 the Pu uncertainty slightly. From Fig. 5, it can be seen that the probability density functions  
 456 from the MCM simulations are symmetrical and not significantly different from a Gaussian  
 457 shape. As such it was possible to express the (relative) standard uncertainty terms by  
 458 dividing the CI from MCM by 2. It is also important to note from these results that the very  
 459 low uncertainty of the  $f$  term (below 0,001% at  $k=1$ ) as calculated by the MCM approach,  
 460 corroborates the hypothesis that its variability could be neglected during the GUM  
 461 calculations.

462 Based on these results, it is possible to say that the MCM approach appears to be a powerful  
 463 tool for the determination of uncertainties on Pu concentration analysis through CPC  
 464 titration.

465

466 **Trueness analysis**

467 The Pu mass fraction determined by using Eq. (10) for each of the 5 replicates, is reported  
 468 in Table 9.

Exp	$m_{Pu}$ (mg)	$m_{sample}(g)$	[Pu] (g/kg)
LF04	6.29518	4.22942	5.5343
LF05	6.27852	4.22274	5.5284
LF06	6.31913	4.24528	5.5347
LF07	6.29521	4.23475	5.5274
LF08	6.29357	4.23285	5.5285
		Mean value	5.5307
		Standard uncert.	0.0035

469 **Table 9** Pu mass fraction in g/kg determined from the experimental analyses  
 470 performed

471 The final analysis result was determined from the mean of the 5 replicates and calculated  
 472 to be  $[Pu]_{mean} = 5.5307$  g/kg. The bias on this value was calculated (from Equ. (17)) as  
 473 0.035%.

474

475 
$$bias = \frac{[Pu]_{mean} - [Pu]_{ref}}{[Pu]_{ref}} = \frac{5.5307 - 5.5326}{5.5326} = -0.035\% \quad (17)$$

476 The estimation of the standard uncertainty in condition of repeatability with 5 replicates is  
477 equal to 0.0035 g/kg. This is consistent with the standard uncertainty calculated by the  
478 MCM approach which is 0.0023 g/kg and can be used to estimate the trueness of the  
479 method.

480 The significance of the method's bias was then analyzed through the normalized deviation  
481 term,  $E_n$ , as shown in Eq. (18) (where  $[Pu]_{ref} = 5.5326$  g/kg,  $u_{ref} = 0.0033$  g/kg, and  $u_{exp} =$   
482  $0.0023$  g/kg). If  $E_n$  is lower than 2 in absolute value, the bias is considered non-significant.

483 
$$E_n = \frac{[Pu]_{mean} - [Pu]_{ref}}{\sqrt{u_{exp}^2 + u_{ref}^2}} \quad (18)$$

484 In our case, this calculation gives:

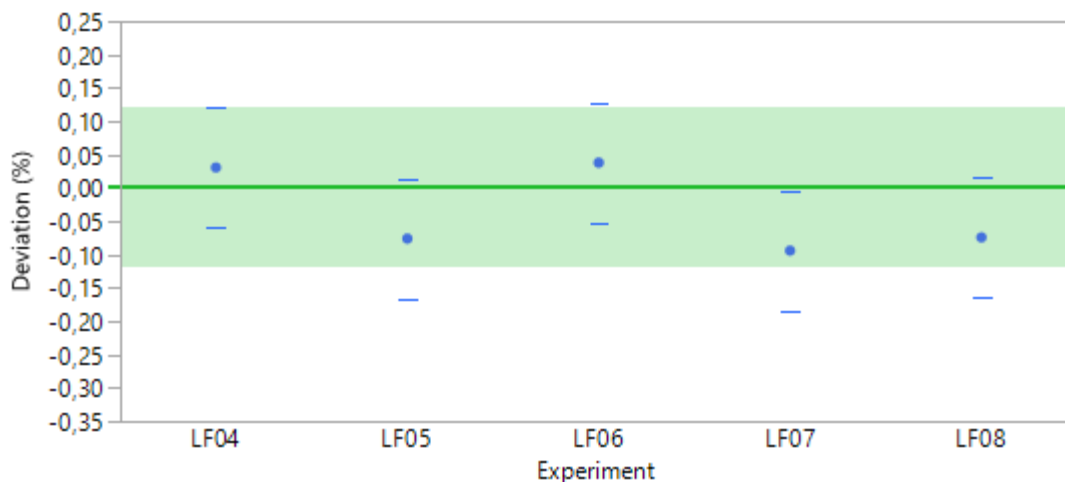
485 
$$|E_n| = \frac{|5.5307 - 5.5326|}{\sqrt{0.0023^2 + 0.0033^2}} = 0.5 < 2$$

486 As such, no bias is observed for the result corresponding to the mean of 5 replicates. The  
487 CPC method can thus be considered a true method for the determination of Pu mass  
488 fraction.

#### 489 Final expression of the result

490 The results for the determinations of Pu mass fraction in the experiments LF04 – LF08  
491 with their expanded uncertainties are shown in Fig. 6 in relation to the known reference  
492 value (and its uncertainty).

493



494

495 **Fig. 6** Plot of the results of the CPC titrations of the EQRAIN Pu 14 solution in terms of  
 496 deviation from the reference value (solid line). The confidence intervals of the reference  
 497 value (band), and the individual measurements (dashes) are also plotted (k=2)

498 It can be seen from Fig. 6 that the results lie within the confidence interval of the reference  
 499 and on both sides of the reference line, thus demonstrating no significant bias. Furthermore,  
 500 the uncertainty of the measurements is of the same order of magnitude to that of the  
 501 reference, indicating that the coulometric method is a suitable technique for the verification  
 502 of reference values during the certification process of RM.

503 From these studies, the final expression of the analysis results is taken as the arithmetic  
 504 mean of the 5 measurements combined with the expanded uncertainty, equivalent to the  
 505 uncertainty calculated by MCM (in a conservative approach, it was chosen not to divide  
 506 by the square root of 5<sup>1</sup>).

507 
$$[Pu] = (5.5307 \pm 0.0045)g/kg \quad (k=2)$$

508 Coulometry performance evaluation at the LAMMAN and comparison to  
 509 ITVs

510 As was reported in Table 10, the relative uncertainty from MCM estimations for the CPC  
 511 titration method performed at the LAMMAN on pure nitrate solutions was calculated to be

---

<sup>1</sup>The uncertainty in this case has not been divided by the square root of the number of replicates because the replicates are based on the same calibration and are not strictly independent measurements: it is a conservative position.



512 0.082% ( $k=2$ ). This uncertainty can be compared to the data taken from the IAEA's ITVs  
513 2010 [1] wherein the  $ITV = 0.14\%$ . The LAMMAN's performance in the field of  
514 coulometry applied to the metrology of Pu is lower than the corresponding ITV because  
515 measurements are done in pure nitrate solutions in ideal laboratory conditions but are  
516 nevertheless consistent with the international expectations established by the ITVs 2010.  
517 This result confirms the role of such a technique for the highly accurate determination of  
518 Pu amounts, which is needed in the case of certification of RMs.

## 519 **Conclusion**

520 The present study details the state of art in the practice of highly accurate CPC at the  
521 CETAMA's LAMMAN. It provides information about the way in which CPC experiments  
522 are performed as well as how the uncertainty of analytical measurements is estimated. Two  
523 methodologies were applied and compared: the classical GUM approach and the Monte  
524 Carlo Method. The two approaches gave comparable values. However, the MCM  
525 calculations were found to give a finer estimation of the distribution of probability of  
526 nonlinear expressions such as the concentration of Pu and the fraction of material  
527 electrolyzed without requiring the application of simplifying assumptions.

528 Considering the promising results, the MCM method will be adopted in the future for our  
529 protocol on the evaluation of uncertainty measurements for coulometric measurements.  
530 This is also possible due to the availability of commercial software powerful enough to  
531 perform the taxing calculations required by the MCM simulations.

532 Finally, it is important to note that the performances reached by the LAMMAN for the  
533 coulometric analysis of pure nitrate solutions are consistent with the IAEA International  
534 Target Values. These results confirm the importance of the analytical technique for the  
535 production of certified RMs.

536 As the CETAMA is now in capacity of producing certified RMs of mixed  
537 uranium/plutonium pure nitrate solutions (named EQRAIN(U+Pu) ), future research on the  
538 technique will focus the applicability of CPC and its implementation for the determination  
539 of Pu in presence of large amounts of uranium.

540       **References**

- 541       1. Zhao K, Penkin M, Norman C, et al (2010) International Target Values 2010 for  
542       Measurement Uncertainties in Safeguarding Nuclear Materials - report number  
543       IAEA-STR-368. IAEA, International Atomic Energy Agency (IAEA), Vienna  
544       (Austria)
- 545       2. Macdonald A, Savage DJ (1979) Plutonium accountancy in reprocessing plants by  
546       ceric oxidation, ferrous reduction and dichromate titration. - report number IAEA-  
547       AM-231/52. IAEA
- 548       3. Ruas A, Leguay N, Sueur R, et al (2014) High accuracy plutonium mass  
549       determination by controlled-potential coulometry. *Radiochim Acta* 102:691–699.  
550       <https://doi.org/10.1515/ract-2013-2213>
- 551       4. Momotov VN, Erin EA (2017) Coulometric methods for uranium and plutonium  
552       determination. *Radiochemistry* 59:1–25.  
553       <https://doi.org/10.1134/S1066362217010015>
- 554       5. Nuclear fuel technology - Controlled-potential coulometric assay of plutonium , ISO  
555       12183:2018
- 556       6. Clark DL (2019) Plutonium handbook, 2nd edition. American Nuclear Society, La  
557       Grange Park, Illinois, USA
- 558       7. Harrar JE (1987) Analytical controlled-potential coulometry. *TrAC Trends Anal*  
559       *Chem* 6:152–157. [https://doi.org/10.1016/0165-9936\(87\)80010-9](https://doi.org/10.1016/0165-9936(87)80010-9)
- 560       8. Holland MK, Weiss JR, Pietri CE (1981) A reference method for the determination  
561       of Plutonium using controlled potential coulometry. *Proc 3rd ESARDA Symp*  
562       *Safeguards Nucl Mater Manag Karlsr Ger*
- 563       9. Newell DB, Cabiati F, Fischer J, et al (2018) The CODATA 2017 values of  $h$  ,  $e$  ,  $k$  ,  
564       and  $N_A$  for the revision of the SI. *Metrologia* 55:L13–L16.  
565       <https://doi.org/10.1088/1681-7575/aa950a>
- 566       10. (2008) Evaluation of measurement data – Guide to the expression of uncertainty in  
567       measurement (GUM), report number JCGM 100:2008. Joint committee for guides in  
568       metrology
- 569       11. (2008) Evaluation of measurement data – Supplement 1 to the “Guide to the  
570       expression of uncertainty in measurement” - Propagation of distributions using a  
571       Monte Carlo method, report number JCGM 101. Joint committee for guides in  
572       metrology
- 573       12. Borges PP, da Silva WB (2014) Metrological evaluation of the certification of  
574       primary reference materials characterized by high-precision constant-current

- 575 coulometry for the reliability of the titration analyses. *J Appl Electrochem* 44:1411–  
576 1420. <https://doi.org/10.1007/s10800-014-0768-x>
- 577 13. (1999) Standard test method for plutonium by controlled-potential coulometry,  
578 ASTM C 1108-99. ASTM International, West Conshohocken, PA.
- 579 14. Holland MK, Cordaro JV (2009) Mass measurement uncertainty for plutonium  
580 aliquots assayed by controlled-potential coulometry. *J Radioanal Nucl Chem*  
581 282:555–563. <https://doi.org/10.1007/s10967-009-0173-9>
- 582 15. Milyukova MS, Gusev NI, Sentyurin IS (1967) Analytical Chemistry of Plutonium.  
583 Wiener Bindery Ltd, Jerusalem
- 584 16. Shults W (1963) Applications of controlled-potential coulometry to the determination  
585 of plutonium. *Talanta* 10:833–849. [https://doi.org/10.1016/0039-9140\(63\)80244-1](https://doi.org/10.1016/0039-9140(63)80244-1)
- 586 17. Holland MK, Weiss JR, Pietri CE (1978) Controlled-potential coulometric  
587 determination of plutonium. *Anal Chem* 50:236–240.  
588 <https://doi.org/10.1021/ac50024a018>
- 589 18. Georgette S, Picart S, Bouyer C, et al (2014) Study of the plutonium (IV)  
590 electrochemical behavior in nitric acid at a platinum electrode. Application to the  
591 cathodic reduction of Pu(IV) in a plate electrolyzer. *J Electroanal Chem* 727:163–  
592 170. <https://doi.org/10.1016/j.jelechem.2014.06.015>
- 593 19. Fallet A, Larabi-Gruet N, Jakab-Costenoble S, Moisy P (2016) Electrochemical  
594 behavior of plutonium in nitric acid media. *J Radioanal Nucl Chem* 308:587–598.  
595 <https://doi.org/10.1007/s10967-015-4423-8>
- 596 20. Bard AJ, Faulkner LR (1980) Electrochemical methods: fundamentals and  
597 applications. Wiley, New York
- 598 21. Audouin P (1981) Controlled potential coulometry: study of the method and its  
599 application, Report number CEA-R-5117. CEA
- 600 22. Leguay N (2011) Plutonium titration by controlled potential coulometry, Report  
601 number CEA-R-6264. CEA
- 602 23. Plutonium metal MP2, Reference Material Certificate. CETAMA
- 603 24. Cox M, Harris P, Siebert BR-L (2003) Evaluation of Measurement Uncertainty  
604 Based on the Propagation of Distributions Using Monte Carlo Simulation. *Meas Tech*  
605 46:824–833. <https://doi.org/10.1023/B:METE.0000008439.82231.ad>
- 606 25. Cox MG, Siebert BRL (2006) The use of a Monte Carlo method for evaluating  
607 uncertainty and expanded uncertainty. *Metrologia* 43:S178–S188.  
608 <https://doi.org/10.1088/0026-1394/43/4/S03>